# Analysis and Evaluation of a Lossless Turn-On Snubber

Hanan Levy, Isaac Zafrany, Gregory Ivensky and Sam Ben-Yaakov*

Tel: +972-7-6461561; Fax: +972-7-6472949; Email: sby@bguee.bgu.ac.il
Power Electronics Laboratory
Department of Electrical and Computer Engineering
Ben-Gurion University of the Negev
P. O. Box 653, Beer-Sheva 84105, ISRAEL

***Abstract*** **- A lossless turn-on snubber was studied analytically, by simulation and experimentally. Limits were found for the proper operation of the snubber and are expressed as permissible duty cycle as a function of input current. It was found that a modified version of the snubber, which includes a tapped main inductor, improves the performance by allowing a wider operational range. The experimental results confirm the theoretical analysis. A reduction of power losses of about 19W was observed when the snubber was implemented in a 1kW Boost converter.**

## I. INTRODUCTION

The recent technological strive toward smaller and lighter systems imposes an ever increasing demand for the reduction of size and weight of inverters and converters while keeping down the overall power loss. This implies high switching frequencies coupled with soft switching schemes to reduce switching losses. Among the possible solutions for soft switching are the dual switch approaches that apply an auxiliary switch to help smooth the transitions of the main switch [1,2]. While these solutions are effective in reducing switching losses [3], they are too costly for many high volume applications. The present relentless competition in the power electronics industry calls for simple and inexpensive solutions to make the design cost effective. Among the possible approaches for soft switching is the lossless snubber technology [4-6] which appears to be less costly than the active snubbers. In this study we analyzed and evaluated experimentally a turn-on lossless snubber that was recently proposed [7]. The objective was to gain a better understanding of the operational modes of the snubber, to drive design guidelines and to verify the theory against experimental results.

## II. PRINCIPLE OF OPERATION

In one embodiment of the turn-on snubber (Fig. 1), it comprises a series inductor ($L_S$), a snubbing capacitor ($C_S$) and two bypass diodes $D_1$ and $D_2$. The function of the

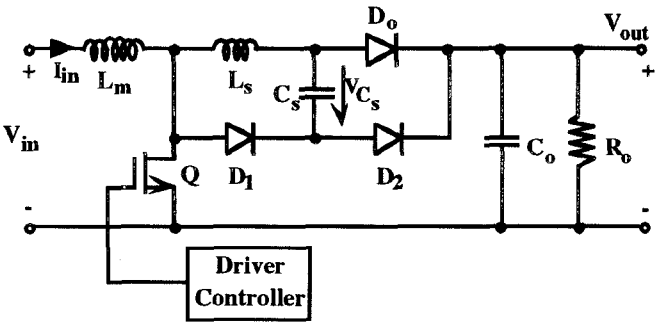


Fig. 1. The lossless turn-on snubber (uncoupled inductors version) implemented in a Boost converter.

inductor is to control the reverse recovery process of the main diode ($D_O$). $C_S$ and the bypass diodes are used to recover the energy trapped in $L_S$. Also, $D_1$ and $D_2$ clamp the switch voltage to $V_{out}$. The operation of the lossless snubber will be discussed in relation to the waveforms of Fig. 2 that were obtained by PSPICE (MicroSim Inc.) simulations.

The operation of the lossless snubber includes six stages (Fig. 2):

1. The first interval commences when the main transistor Q turns on. The current through $D_O$ and $L_S$, which starts as $I_{in}$, decreases linearly to zero, changes polarity and then increases (amplitude wise) linearly until it reaches its maximum (negative) value $I_{rm}$ at time $t_1$.

The duration of interval $t_0$-$t_1$ is found to be:

$$t_{0\text{-}1} \cong \frac{I_{in}L_s}{V_{out}} + t_{rm} \qquad (1)$$

where $t_{rm}$ defined as the duration until the peak reverses current is reached. The magnitude of the reverse recovery current can be approximated by:

$$I_{rm} = \frac{V_{out}t_{rm}}{L_s} \qquad (2)$$

Hence

$$t_{0\text{-}1} \cong t_{rm}\frac{a}{1+a} \qquad (3)$$

* Corresponding author.

where

$$a = \frac{I_{rm}}{I_{in}} \qquad (4)$$

2. Once the main diode $D_O$ is cut off, the inductor $L_S$ and capacitor $C_S$ are free to resonate in the interval $t_1$-$t_2$.

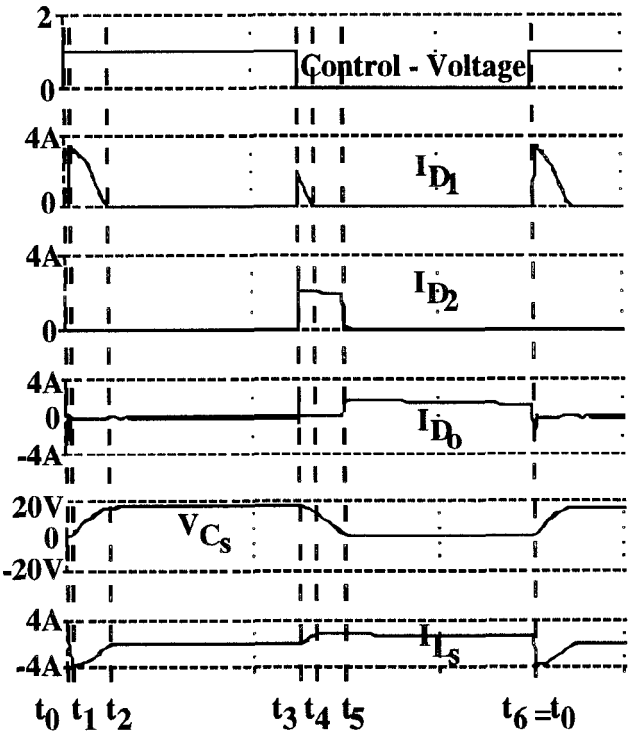


Fig. 2. Basic waveforms of the lossless snubber of Fig. 1.

The diode $D_1$ closes the path of the resonant current of $L_SC_S$ and carries the cosinusoidal current that develops. The magnitude of the resonant current and the capacitor $C_S$ voltage can be expressed as:

$$i_{Ls}(t) = I_{rm} \cos(\omega_r t) \qquad (5)$$

$$v_C(t) = \frac{I_{rm}}{\omega_r C_S} \sin(\omega_r t) \qquad (6)$$

where:

$$\omega_r = \frac{1}{\sqrt{L_S C_S}} \qquad (7)$$

t is time, accounted from the beginning of each interval.

The interval $t_1$-$t_2$ ends when the current of $D_1$ reaches zero. Consequently, the duration of interval $t_1$-$t_2$ is found to be:

$$t_{1\text{-}2} = \frac{T_r}{4} \qquad (8)$$

where $T_r = \frac{2\pi}{\omega_r}$ is the resonant period. The voltage across the capacitor $C_S$ at this instance is:

$$V_{Cmax} = V_{out} t_{rm} \omega_r \qquad (9)$$

3. During the interval $t_2$-$t_3$ the main inductor ($L_m$) charges, diode $D_1$ is off and the voltage across the capacitor $C_S$ is equal to $V_{Cmax}$ (Fig. 2).

4. The interval $t_3$-$t_4$ starts when Q turns 'off'. Diodes $D_1$ and $D_2$ are immediately clamped to $V_{out}$ while carrying $I_{in}$. The resonant circuit $L_SC_S$ is now shorted by the conducting $D_1$ and the current $i_{Ls}$ will increase under action of $v_C$ until it will reach $I_{in}$. The current of $D_1$ is now the difference between $i_{Ls}$ and $I_{in}$. The magnitude of the resonant current and the capacitor $C_S$ voltage during this interval can be expressed as:

$$i_{Ls}(t) = I_{rm} \sin(\omega_r t) \qquad (10)$$

$$i_{in}(t) = I_{in\ pk} - \frac{V_{out}-V_{in}}{L_m} t \qquad (11)$$

where in Boost topology:

$$I_{in\ pk} = I_{in\ av} + \frac{V_{in} D T_s}{2L_m} \qquad (12)$$

$I_{in\ av}$ is the average input current, D is the duty cycle and $T_s$ is the switching period.

This interval ends when $i_{Ls}(t_4) = i_{in}(t_4)$ and the current of $D_1$ smoothly reaches zero, turning it off. Approximately

$$t_{3\text{-}4} = \frac{1}{\omega_r} \sin^{-1}\left(\frac{I_{in\ pk}}{I_{rm}}\right) \qquad (13)$$

The magnitude of the input current and the capacitor $C_S$ voltage at this moment can be expressed as:

$$i_{in}(t_4) = i_{Ls}(t_4) = \frac{V_{Cmax}}{\sqrt{\frac{L_s}{C_s}}} \sin(\omega_r t_4) \qquad (14)$$

$$v_C(t_4) = V_{Cmax} \cos(\omega_r t_4) \qquad (15)$$

5. In the interval $t_4$-$t_5$ the input current $i_{in}$ flows through $L_S$, $C_S$ and $D_2$ until $v_C(t)$ reaches zero. In this moment ($t_5$), $D_O$ will turn-on and $D_2$ will turn-off. The duration of interval $t_4$-$t_5$ can be approximated by :

$$t_{4\text{-}5} = \frac{C_S v_C(t_4)}{I_{in\ pk}} \qquad (16)$$

6. In the final operational stage $t_5$-$t_6$, $L_S$ and $D_O$ are conducting while the auxiliary diodes are turned off. This interval ends at $t_6$ (or $t_0$ )when the transistor turns-on.

Note that the operating conditions of the snubber described above are for the case:

$$I_{in\ pk} \le I_{rm} \quad (17)$$

If $I_{in\ pk} > I_{rm}$ the conduction interval of $D_1$ is much longer because the commutation process from the diode $D_1$ to the inductor $L_s$ acts only under the influence of the on-voltage of the diode after the voltage across the capacitor $C_s$ gets zero.

## III. THE COUPLED INDUCTOR REALIZATION

A second, more desirable embodiment of the lossless snubber is depicted in Fig. 3. In this case, the main inductor is tapped, adding thereby a positive or negative voltage to $L_s$ (Fig. 4).

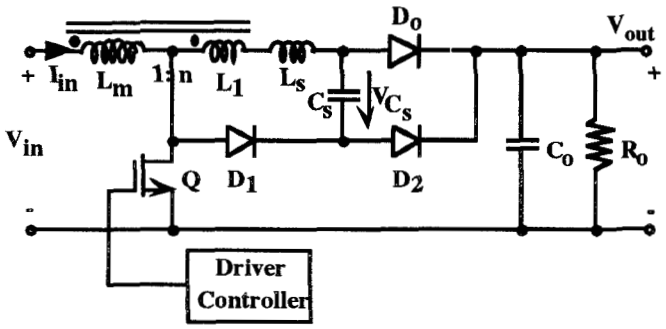


Fig. 3. The lossless turn-on snubber (coupled inductors version) implemented in a Boost converter.

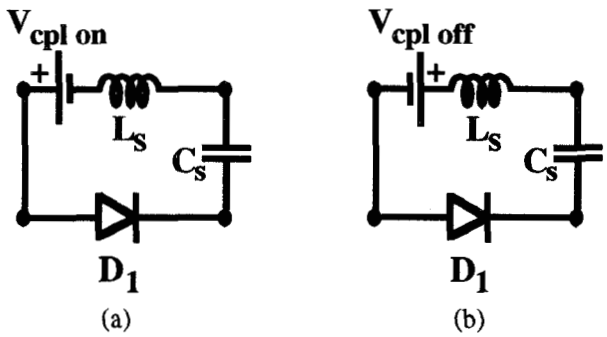


Fig. 4. Simplified equivalent circuits of the resonant elements when the transistor is 'on' (a) and when the transistor is 'off' (b)

For a tap to main inductor turn ratio of n, the magnitude of the added voltages can be estimated from:

$$V_{cpl\ on} = nV_{in} \quad (18)$$

$$V_{cpl\ off} = n\,(V_{out} - V_{in}) \quad (19)$$

Consequently, the maximal reverse current of the main diode ($D_0$) will be in this case:

$$I_{rm} = \frac{(V_{out}+V_{cpl\ on})\,t_{rm}}{L_s} \quad (20)$$

The duration of the interval $t_0$-$t_1$ can be obtained as before by (3).

The resonant inductor current $L_s$ and capacitor voltage $C_s$ at turn-on during the interval $t_1$-$t_2$ will be:

$$i_{Ls}(t) = I_{rm}\cos(\omega_r t) + \frac{V_{cpl\ on}}{\sqrt{\frac{L_s}{C_s}}}\sin(\omega_r t) \quad (21)$$

$$v_C(t) = I_{rm}\sqrt{\frac{L_s}{C_s}}\sin(\omega_r t) + V_{cpl\ on}(1-\cos(\omega_r t)) \quad (22)$$

This interval ends at $t_2$ when the current $i_{L_s}$ reaches zero. Consequently, the duration of $t_1$-$t_2$ interval will be:

$$t_{1\text{-}2} = \frac{1}{\omega_r}\left[\tan^{-1}\left(-\frac{I_{rm}\sqrt{\frac{L_s}{C_s}}}{V_{cpl\ on}}\right) + \pi\right] \quad (23)$$

The relationship (23) is depicted in Fig. 5 where

$$I^*_{rm} = I_{rm}\frac{\sqrt{\frac{L_s}{C_s}}}{V_{out}} \quad (24)$$

$$V^*_{cpl\ on} = \frac{V_{cpl\ on}}{V_{out}} \quad (25)$$

We see that $t_{1\text{-}2}$ increases with rising $V_{cpl\ on}$.

The capacitor's voltage $v_C(t)$ (eq. (22)) reaches its maximum value $V_{Cmax}$ at the instance $t_2$. The relationship

$$V^*_{Cmax} = \frac{V_{Cmax}}{V_{out}} \quad (26)$$

as a function on $I^*_{rm}$ and $V^*_{cpl\ on}$ is depicted in Fig. 6.
We see that due to the coupling, the voltage across the capacitor gets somewhat larger.

The resonant inductor current $L_s$ and capacitor voltage $C_s$ during the interval $t_3$-$t_4$ will be:

$$i_{Ls}(t) = \frac{V_{C\ max} + V_{cpl\ off}}{\sqrt{\frac{L_s}{C_s}}}\sin(\omega_r t) \quad (27)$$

$$v_C(t) = (V_{Cmax}+V_{cpl\ off})\cos(\omega_r t) - V_{cpl\ off} \quad (28)$$

Two conditions must be checked for finding the end moment $t_4$ of the interval $t_3$-$t_4$:

$$i_{Ls}(t_4') = I_{in\ pk} \quad (29)$$

$$v_C(t_4'') = 0 \quad (30)$$

or applying (27) and (28)

$$t_4' = \sqrt{L_s C_s}\,\sin^{-1}\left(\frac{I_{in\ pk}\sqrt{\frac{L_s}{C_s}}}{V_{Cmax}+V_{cpl\ off}}\right) \quad (31)$$

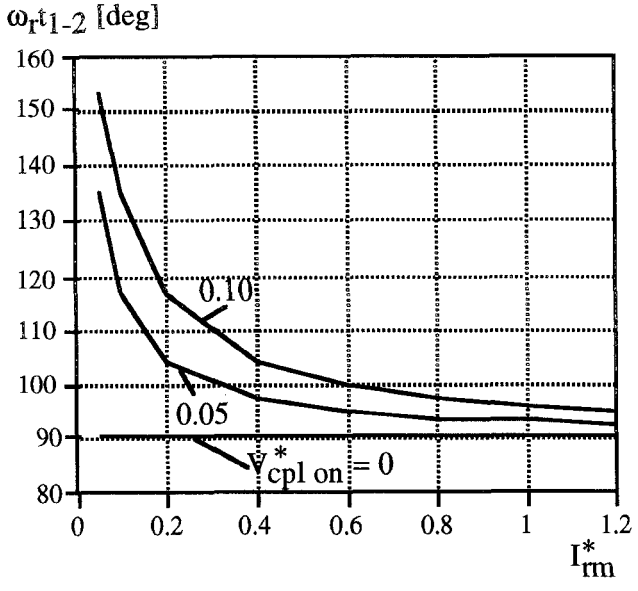


Fig. 5. Duration of the interval $t_{1-2}$ as a function of the peak value of the normalized reverse current $I^*_{rm}$ for different values of the normalized tap voltage $V^*_{cpl\ on}$.

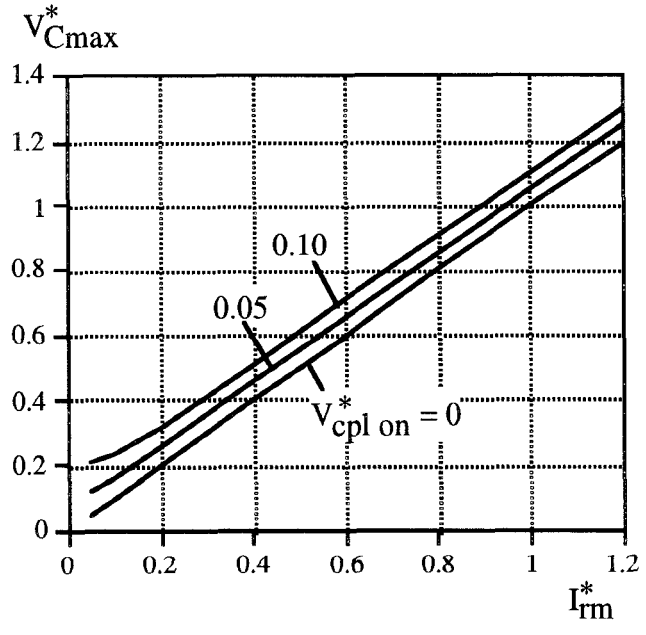


Fig. 6. The peak of the capacitor's voltage $V^*_{Cmax}$ as a function of the peak value of the reverse current $I^*_{rm}$ for different values of normalized tap voltage $V^*_{cpl\ on}$.

$$t_4'' = \sqrt{L_s C_s}\cos^{-1}\left(\frac{1}{\frac{V_{Cmax}}{V_{cpl\ off}}+1}\right) \qquad (32)$$

$t_4$ assumes the value of $t_4'$ or $t_4''$ whichever is smaller. $t_4$ is equal to $t_4''$ in the case

$$I_{in\ pk} > \frac{V_{Cmax}+V_{cpl\ off}}{\sqrt{\frac{L_s}{C_s}}} \qquad (33)$$

when $t_4'$ does not exist.

In the case $t_4=t_4'$, which is denoted as 'Mode 1', the interval $t_4$-$t_5$ is similar to the one described above for the uncoupled snubber (eq. (16)).

Now we study the case $t_4=t_4''$ (Mode 2).

In the interval $t_4$-$t_5$ in Mode 2 the current $i_{Ls}(t)$ is rising linearly under action of $V_{cpl\ off}$:

$$i_{Ls}(t) = i_{Ls}(t_4'') + \frac{V_{cpl\ off}+V_{D1(on)}}{L_s}\,t \qquad (34)$$

$V_{D1(on)}$ is the voltage drop on the conducting diode $D_1$. Its influence is practical insignificant when $V_{cpl\ off} >> V_{D1(on)}$, but in the case $V_{cpl\ off} \approx 0$ its action is very important because without any voltage source in the network the current $i_{Ls}(t)$ would not rise and therefore the diodes $D_1$ and $D_2$ would not be turned off.

The duration of the interval $t_4$-$t_5$ can be estimated by assuming the condition $i_{Ls}(t_5) = I_{in\ pk}$:

$$t_{4-5} = \frac{[I_{in\ pk} - i_{Ls}(t_4'')]L_s}{V_{cpl\ off}+V_{D1(on)}} \qquad (35)$$

The last equation clearly shows the benefit of coupling: $t_{4-5}$ decreases when $V_{cpl\ off}$ is larger. This decreases the minimum permissible value of the turn-off interval of the switch ($t_{off\ min}$) and therefore increases the maximum acceptable value of the duty cycle for proper operation

$$D_{max} = 1 - \frac{t_{off\ min}}{T_s} \qquad (36)$$

## IV. LIMITATIONS

To insure complete discharge of $C_s$ before next 'turn-on', the criteria below should be satisfied:

$$t_{off} > t_{3-4} + t_{4-5} \qquad (37)$$

i. e. the minimum value of the turn-off interval of the switch must conform to:

$$t_{off\ min} = t_{3-4} + t_{4-5} \qquad (37a)$$

We find $t_{off\ min}$ in Mode 1 under assumption: $V_{cpl\ off}/V_{out} = 0$. The error due to this assumption is practically insignificant because the duty cycle corresponding to $t_{off\ min}$ is high and therefore $V_{in} \approx V_{out}$, $V_{cpl\ off}=n(V_{out}-V_{in}) \approx 0$. From (31), (16) and (28) we obtain:

$$(\omega_r t_{off\ min})_{M1}=\sin^{-1}\left(\frac{I^*_{in\ pk}}{V^*_{Cmax}}\right)+\frac{V^*_{Cmax}}{I^*_{in\ pk}}\cos(\omega_r t_4) \quad (38)$$

where

$$I^*_{in\ pk} = I_{in\ pk}\frac{\sqrt{\frac{L_s}{C_s}}}{V_{out}} \quad (39)$$

The relationship (38) is depicted in Fig. 7. We see that $(\omega_r t_{off\ min})_{M1}$ decreases when $\frac{I^*_{in\ pk}}{V^*_{Cmax}}$ becomes higher.

Optimum values are when $\frac{I^*_{in\ pk}}{V^*_{Cmax}} > 0.7$. Note that in Mode 1 $I^*_{in\ pk} / V^*_{Cmax} < 1$.

We find $t_{off\ min}$ in Mode 2 in the case

$$I^*_{in\ pk} > V^*_{Cmax} + V^*_{cpl\ off}$$

under the assumption: $V_{cpl\ off} << V_{Cmax}$.

Applying (32), (35) and (27) we obtain:

$$(\omega_r t_{off\ min})_{M2} = \frac{\pi}{2} - 1 + \frac{V^*_{Cmax}}{V^*_{cpl\ off}}\left(\frac{I^*_{in\ pk}}{V^*_{Cmax}} - 1\right) \quad (40)$$

The relationship (40) is depicted on Fig. 8. It shows that $(t_{off\ min})_{M2}$ is increasing linearly with $\frac{I^*_{in\ pk}}{V^*_{Cmax}}$. Optimal ratios of $\frac{I^*_{in\ pk}}{V^*_{Cmax}}$ are near 1.0 when $(t_{off\ min})_{M2}$ is about 95-100°.

The minimum admissible value of the turn on interval of the switch is obtained from (3), (4) and (23):

$$t_{on\ min} = t_{0\text{-}1}+t_{1\text{-}2} =$$

$$= t_{rm}\frac{a}{1+a} + \frac{1}{\omega_r}\left[\tan^{-1}\left(-\frac{a\, I_{in}\sqrt{\frac{L_s}{C_s}}}{V_{cpl\ on}}\right)+\pi\right] \quad (41)$$

Analysis of (41) and Fig. 5 show that $t_{on\ min}$ increases with rising $V_{cpl\ on}$. Accordingly grows the minimum admissible value of the duty cycle

$$D_{min} = \frac{t_{on\ min}}{T_s} \quad (42)$$

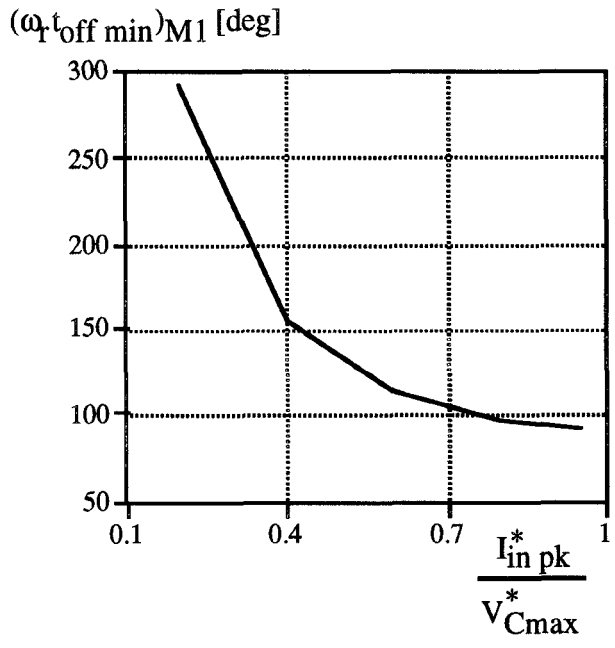


Fig. 7. The minimum acceptable value of the switch turn-off interval in Mode 1. $(\omega_r t_{off\ min})_{M1}$ as a function of the ratio $I^*_{in\ pk}/V^*_{Cmax}$.

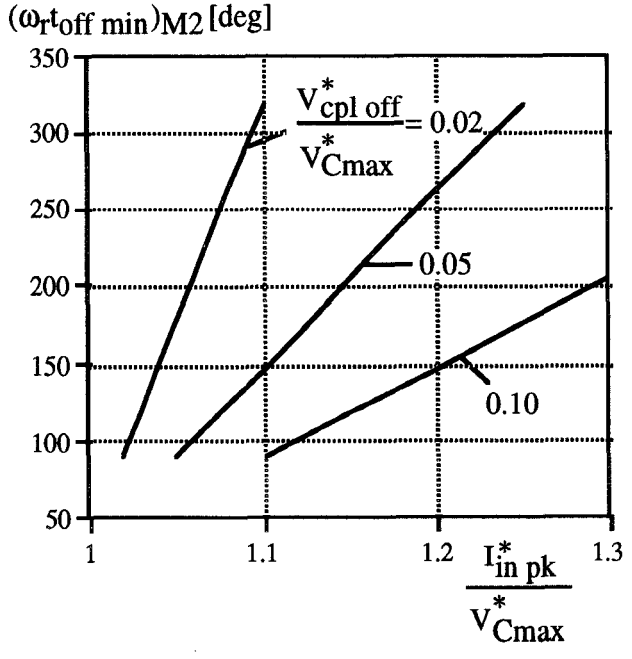


Fig. 8. The minimum acceptable value of the switch turn off interval in Mode 2. $(\omega_r t_{off\ min})_{M2}$ as a function of the ratio $I^*_{in\ pk}/V^*_{Cmax}$ by different values of $V^*_{cpl\ off}/V^*_{Cmax}$.

## V. COMPONENT STRESSES

The current and voltage stresses of the components of the snubber are given in Table I where

$$I_{pk\ sn} = I_{rm} + \frac{V_{cpl\ on}}{\sqrt{\frac{L_s}{C_s}}} \quad (43)$$

$$V_{Cmax} = I_{rm}\sqrt{\frac{L_s}{C_s}} + 2V_{cpl\ on} \quad (44)$$

$$D = \frac{t_{on}}{T_s} \quad (45)$$

$$D_{off} = 1 - D \quad (46)$$

$I_{rm}$ - see eq. (20); $V_{cpl\ on}$ - (18); $V_{cpl\ off}$ - (19); $t_{3\text{-}4}$ - (31) or (32); $t_{3\text{-}5}$ - (38) or (40), $\omega_r$ - (7).

| | $I_{pk}$ | $I_{rms}$ | $I_{av}$ | $V_{max}$ |
|---|---|---|---|---|
| $L_s$ | $I_{pk\ sn}$ | $I_{in}\sqrt{D_{off}}$ | | |
| $C_s$ | $I_{pk\ sn}$ | $I_{in}\sqrt{\frac{t_{3\text{-}5}}{T_s}}$ | | $V_{Cmax}$ |
| $D_1$ | $I_{pk\ sn}$ | | $\frac{I_{pk\ sn}}{2\pi}\frac{T_r}{T_s} + I_{in}(t_{3\text{-}4}/T_s)$ | $V_{Cmax} + V_{cpl\ off}$ |
| $D_2$ | $I_{in}$ | | $I_{in}\frac{t_{3\text{-}5}}{T_s}$ | $V_{out}$ |
| $D_o$ | $I_{pk\ sn}$ | | $I_{in}D_{off}$ | $V_{Cmax} + V_{out}$ |
| Q | $I_{in}$ | $I_{in}\sqrt{D}$ | | $V_{out}$ |

Table I. Current and voltage stresses of the snubber components.

## VI. EXPERIMENTAL RESULTS

The proposed lossless turn-on snubber was tested experimentally to examine its operation and to assess the reduction in switching losses. The measured waveforms (Fig. 9) were found to be in excellent agreement with the simulated ones.

The heat dissipation process of the experimental system was calibrated by correlating the temperature rise of the heat sink to the total power losses (Fig. 10). The parameters of the Boost converter were as follows:

$V_{in}$=200V; $V_{out}$=400V; $P_{in}$=1000W; $C_s$=100nF; $L_s$=3μH; $f_s$ = 100kHz; n=1/7; reverse recovery time of the main diode $t_{rr}$=60nS.

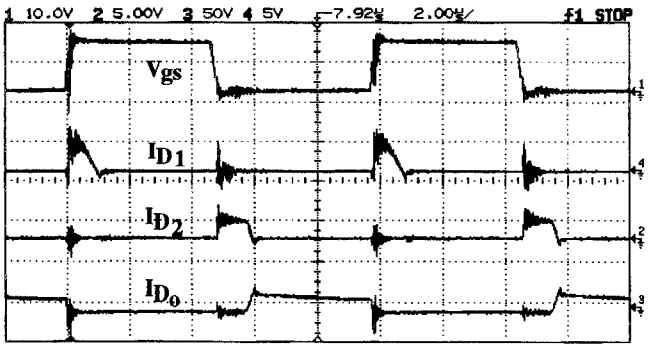


Fig. 9. Experimental waveforms. Compare to Fig. 2.

Temperature rise without snubber was measured to be $\Delta T = 26^0C$ which implies (Fig. 10) that total power dissipation was about $P_{dissipated}$=48.81W. Temperature rise with the snubber was $\Delta T = 16^0C$ which implies total losses of $P_{dissipated}$=29.21W. That is, by applying the proposed lossless turn-on snubber, the power dissipation dropped by 19.6W.

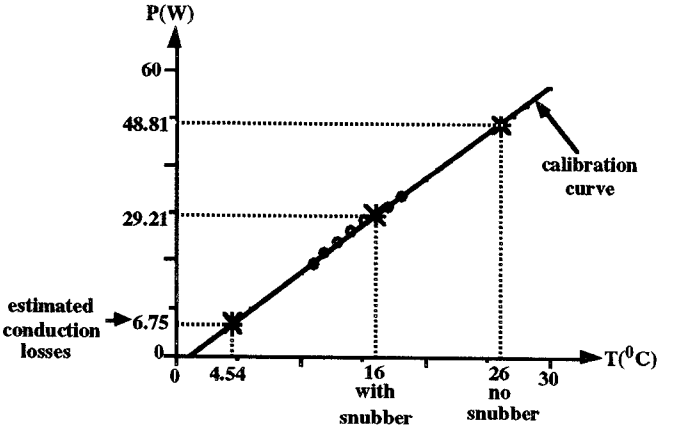


Fig. 10. Calibration curve of temperature rise of heat sink above ambient and experimental points.

## VII. CONCLUSIONS

The lossless turn on snubber analyzed and evaluated in this study appears to be a viable choice for practical designs. The main disadvantage of the snubber is the limitation of the duty cycle range. In active power factor corrector, maximum current coincides with maximum input voltage, i.e. minimum duty cycle. Consequently, the output voltage should be adjusted such that even for the highest line voltage expected, D should be above $D_{min}$. Otherwise $L_s$ will not have sufficient time to discharge. This might lead to a failure. Another point to be observed is the possibility of $D_1$, $D_2$ conducting during the $t_{off}$ period. This will increase losses and may cause hard switching at turn-on. The detailed analysis

presented here and the mathematical relationships derived, provide a comprehensive information required for a reliable design. The proposed snubber was implemented in a commercial product and proved to increase the overall efficiency by 1%-2% at power levels of 1.5KW. An extra benefit of the snubber is the reduction of EMI associated with the reverse recovery of the main diode.

## APPENDIX
## SIMPLIFIED DESIGN GUIDELINES

The following procedure is suggested for the practical design of a turn-on lossless snubber implemented in a Boost converter.

It is assumed that the following parameters are given: maximum input (average) current of the converter ($I_{in\ max}$), minimum and maximum input voltage ($V_{in\ min}$, $V_{in\ max}$), output voltage ($V_{out}$), main inductance ($L_m$) and reverse recovery time ($t_{rr}$) of the main diode $D_0$.

1. Select the switching frequency $f_s$ according to the converter's component values available.
2. Calculate the maximal and minimal values of the duty cycle corresponding to $V_{in\ min}$ and $V_{in\ max}$:
$$D_{max} = 1 - \frac{V_{in\ min}}{V_{out}} \quad ; \quad D_{min} = 1 - \frac{V_{in\ max}}{V_{out}}$$
3. Calculate minimal values of the turn on and turn off intervals of the switch:
$$t_{on\ min} = \frac{D_{min}}{f_s} \quad ; \quad t_{off\ min} = \frac{1}{f_s}(1 - D_{max})$$
4. Set $(\omega_r t_{off\ min}) \approx 270^o \ldots 360^o$ and calculate the resonant frequency $\omega_r$ using the value of $t_{off\ min}$ from step 3.
5. Determine the magnitude of the reverse recovery current of the diode $D_o$:
$$I_{rm} = a\, I_{in\ max}.$$
It is recommended to choose a = 1.3 , taking into account the effect of a large input ripple current.
6. Calculate approximately $L_S$ neglecting the influence of coupling and assuming that $t_{rm}=t_{rr}$:
$$L_S = \frac{V_{out}\, t_{rr}}{I_{rm}}$$
7. Calculate capacitance $C_s$ using the data from steps 4 & 6:
$$C_S = \frac{1}{\omega_r^2 L_S}$$
8. Calculate the maximal peak value of the input current .
9. Set $\frac{I^*_{in\ pk}}{V^*_{Cmax}} \approx 0.9 \ldots 1.0$ and using the data of steps 6-8 calculate the peak voltage across the capacitor:
$$V_{Cmax} = \frac{(I_{in\ pk})_{max}\sqrt{\frac{L_S}{C_S}}}{\left(\frac{I^*_{in\ pk}}{V^*_{Cmax}}\right)}$$
10. Calculate normalized peak values of the reverse recovery current and of the voltage across the capacitor:
$$I^*_{rm} = I_{rm}\frac{\sqrt{\frac{L_S}{C_S}}}{V_{out}} \quad ; \quad V^*_{Cmax} = \frac{V_{Cmax}}{V_{out}}$$
11. Find normalized value of the coupling voltage $V^*_{cpl\ on}$ using the plots (Fig. 6) and data of step 10. Note: coupling is not necessary if the point corresponding to the data of step 10 lies below the curve $V^*_{cpl\ on}$ on Fig. 6.
12. Calculate the coupling voltage $V_{cpl\ on} = V^*_{cpl\ on} \cdot V_{out}$ and the necessary turns ratio n :
$$n = \frac{V_{cpl\ on}}{V_{in}}$$
Note: steps 8-11 correspond to the case when the peak of the input current has the highest value.
13. Calculate the minimal admissible value of the turn on interval of the switch $t_{on\ min}$ putting $(V_{cpl\ on})_{Dmin}$ in (41) and compare the result with the value of $t_{on\ min}$ from step 3. In the case $(t_{on\ min})_{step\ 13} > (t_{on\ min})_{step3}$ we must repeat the design with lower resonant frequency $\omega_r$ .
14. Calculate current and voltage stresses of all elements of the snubber and choose these elements.

## REFERENCES


[1] G. Ivensky, D. Sidi and S. Ben-Yaakov, "A soft switcher optimized for IGBTs in PWM topologies", *IEEE APEC Record,* 1995, pp. 900-906.

[2] S. Ben-Yaakov, G. Ivensky, O. Levitin and A. Treiner, "Optimization of the auxiliary switch components in a flying capacitor ZVS PWM converter," *IEEE APEC Record,* 1995, pp. 503-509.

[3] K. M. Smith and K. M. Smedley, "A comparison of voltage mode soft switching methods for PWM converters," *IEEE APEC Record,* 1996, pp. 291-298.

[4] B. W. Williams, *Power Electronics*, McGraw-Hill Book Company, New-York, 1992.

[5] M. S. Vilela, E. A. A. Coelho, J. B. Vieira Jr., L. C. de Freitas, and V. J. Farias, "A family of PWM soft-switching converters with low stresses of voltage and current ," *IEEE APEC Record,* 1996, pp. 299-304.

[6] M. S. Vilela, E. A. A. Coelho, J. B. Vieira Jr., L. C. de Freitas, and V. J. Farias, "PWM soft-switching converters using a single active switch," *IEEE APEC Record,* 1996, pp. 299-304.

[7] I. D. Jitaru, "Soft transitions power factor correction circuit," *Proceedings of HFPC,* May 1993, pp. 202-208.